Computing Sacker-Sell spectra in discrete time dynamical systems

Thorsten Hüls*

Fakultät für Mathematik, Universität Bielefeld
Postfach 100131, 33501 Bielefeld, Germany
huels@math.uni-bielefeld.de

September 1, 2010

Abstract

In this paper we develop boundary value methods for detecting Sacker-Sell spectra in discrete time dynamical systems. The algorithms are advancements of earlier methods for computing projectors of exponential dichotomies. The first method is based on the projector residual $P^2 - P$. If this residual is large, then the difference equation has no exponential dichotomy. Further criterions for detecting Sacker-Sell spectral intervals are the norm of end- and midpoints of the solution of a specific boundary value problem. Refined error estimates for the underlying approximation process are given and the resulting algorithms are applied to an example with known continuous Sacker-Sell spectrum, as well as to the variational equation along orbits of Hénon's map.

Keywords: Sacker-Sell spectrum, Boundary value problem, Exponential dichotomy, Dichotomy projectors.

AMS Subject Classification: 37B55, 37C75, 34D09, 34B05.

1 Introduction

For non-autonomous difference equations of the form

$$u_{n+1} = A_n u_n, \quad n \in \mathbb{Z}$$

*Supported by CRC 701 'Spectral Structures and Topological Methods in Mathematics'.

several characterizations of spectra have been developed in the literature cf. Dieci & Van Vleck (2007) for continuous time systems. In discrete time, a generalization to non-invertible systems in given in Aulbach & Siegmund (2001). Our focus lies on the so called Sacker-Sell spectrum σ_{ED}, which is introduced in Sacker & Sell (1978). Its construction is based on the notion of exponential dichotomies, see Appendix A. This spectrum is the set of values $\gamma > 0$, for which the scaled equation

$$u_{n+1} = \frac{1}{\gamma} A_n u_n, \quad n \in \mathbb{Z} \tag{1}$$

possesses no exponential dichotomy on $\mathbb{Z}$. The complementary set $\mathbb{R}^+ \setminus \sigma_{\mathrm{ED}}$ is called the resolvent set.

In Dieci & Van Vleck (2002), Dieci & Elia (2008) initial value methods, based on the QR-algorithm and the SVD decomposition are applied for computing spectral intervals in continuous time. These techniques are quite efficient for detecting the whole Sacker-Sell spectrum. But if one is interested in analyzing whether (1) has an exponential dichotomy at a given value of γ or for γ in some region of the positive real axis, it seems to much to compute the whole spectrum.

We apply boundary value techniques for computing Sacker-Sell spectral intervals in discrete time. Three tests are proposed; the first one is based on computing the projector residual, while the second and third allow, roughly speaking, to read off from the solution of the specific boundary value problem

$$u_{n+1} = \frac{1}{\gamma} A_n u_n + \delta_{n,N-1} r, \quad n = n_-, \ldots, n_+ - 1, \quad \delta \text{ Kronecker symbol} \tag{2}$$

whether γ lies in a spectral interval or in the resolvent set. Note that the boundary value approach captures in certain respects the global behavior. The solution of (2) sensitively depends on γ, whereas a change of γ leads in the QR-method to a simple shift of intervals.

The algorithms in this paper are based on a direct approach for the numerical computation of dichotomy projectors from Hüls (2009). For extending these results to the Sacker-Sell spectrum, pointwise estimates for the approximation error of the solution of (2) are needed. Corresponding results are stated in Section 2, particularly in case of periodic boundary conditions.

In Section 3, we introduce our algorithms for detecting Sacker-Sell spectral intervals. In a given interval L we choose a grid L_{g} and compute for each $\gamma \in L_{\mathrm{g}}$ a quantity that indicates, whether (1) possesses an exponential dichotomy.

The basis of the first test are approximate dichotomy projectors. We prove that the projector residual $\|P^2 - P\|$ is exponentially small in case of an exponential dichotomy and in reverse, if this expression is large, then the difference equation cannot have a dichotomy. Due to the approximation of the projectors, this approach turns out to be computationally expensive.

In order to reduce the effort, two further tests are developed that are based on solving (2) with the boundary condition

$$u_{n_-} - u_{n_+} = x, \tag{3}$$

where x is a fixed vector of length 1.

Continuous Sacker-Sell spectrum occurs, for example, if the difference equation possesses half-sided dichotomies on $\mathbb{Z}^-$ and $\mathbb{Z}^+$ that cannot be continued to $\mathbb{Z}$. This is either caused by half sided dichotomy projectors of different rank or by a tangential intersection of the range of the unstable projector on $\mathbb{Z}^-$ with the range of the stable projector on $\mathbb{Z}^+$.

The values $\|u_{n_\pm}\|$ at the end points as well as the values $\|u_{n_{1,2}}\|$ at the midpoints $n_{1,2} = \frac{n_\mp + N}{2}$ may be taken as an indicator. We analyze in detail that these quantities are bounded in the resolvent set – those at the midpoints even converge to 0, while they are expected to be large in spectral intervals.

The resulting algorithms are applied to a linear test example with known continuous Sacker-Sell spectrum, caused by half sided projectors of different rank or by tangential intersections. In Section 4, a more realistic example is considered. Spectral intervals of the variational equation along heteroclinic and homoclinic Hénon orbits are computed. For these examples, the variational equation is asymptotically constant. The heteroclinic case exhibits continuous spectrum, while the homoclinic case has point spectrum only. A third example is the variational equation, obtained from a chaotic trajectory on the Hénon attractor. The resulting difference equation, to which we also apply our algorithms, is asymptotically non-constant.

Finally, we compare these results with QR-computations for the same examples, and state a conclusion.

2 Error estimates

An algorithm for computing dichotomy projectors numerically is introduced in Hüls (2009). These results are summarized in this section and refined as well as extended error estimates are developed, particularly for the projector residual and for periodic boundary conditions of the form (3).

Consider the linear difference equation

$$u_{n+1} = A_n u_n, \quad n \in \mathbb{Z}, \tag{4}$$

and denote by Φ its solution operator. For the forthcoming analysis, we assume that this difference equation possesses an exponential dichotomy on $\mathbb{Z}$, see Appendix A.

A1 The difference equation (4) with matrices $A_n \in \mathbb{R}^{k,k}$, having a uniformly bounded inverse, possesses an exponential dichotomy on $\mathbb{Z}$ with data $(K, \alpha_s, \alpha_u, \bar{P}^s_n, \bar{P}^u_n)$.

The computation of dichotomy projectors is based on solving the inhomogeneous linear system

$$u^i_{n+1} = A_n u^i_n + \delta_{n,N-1} e_i, \quad n \in \mathbb{Z}, \quad e_i \; i\text{-th unit vector.} \tag{5}$$

Using Green's function, cf. Palmer (1988), the unique bounded solution $\bar{u}_{\mathbb{Z}}$ of (5) has the explicit form

$$\bar{u}^i_n = G(n,N)e_i, \; n \in \mathbb{Z}, \quad \text{where} \quad G(n,m) = \begin{cases} \Phi(n,m)\bar{P}^s_m, & n \geq m, \\ -\Phi(n,m)\bar{P}^u_m, & n < m, \end{cases}$$

and consequently

$$\bar{P}^s_N = \left(\bar{u}^1_N, \ldots \bar{u}^k_N\right). \tag{6}$$

In numerical computations, one restricts equation (5) to a finite interval $J = [n_-, n_+] \cap \mathbb{Z}$. In Hüls (2009) the following approaches are discussed:

(1) A boundary value ansatz

$$\begin{aligned} u_{n+1} &= A_n u_n + \delta_{n,N-1} r, \quad n = n_-, \ldots, n_+ - 1, \\ b(u_{n_-}, u_{n_+}) &= 0, \end{aligned} \tag{7}$$

with periodic or projection boundary conditions b, defined as

$$b_{\text{per}}(x,y) := x - y, \tag{8}$$

$$b_{\text{proj}}(x,y) := \begin{pmatrix} Y_s^T x \\ Y_u^T y \end{pmatrix}, \tag{9}$$

where the columns of Y_s and Y_u form a basis of $\mathcal{R}(Q^u)^\perp$ and $\mathcal{R}(Q^s)^\perp$. Q^s and Q^u are two complementary projectors, having the same rank as the stable and unstable dichotomy projectors $\bar{P}^s_n$ and $\bar{P}^u_n$, respectively. Well posedness requires for periodic boundary conditions (8) the angle condition

$$\measuredangle(\mathcal{R}(\bar{P}^s_{n_-}), \mathcal{R}(\bar{P}^u_{n_+})) \geq \sigma \tag{10}$$

and for projection boundary conditions (9), we assume that

$$\measuredangle(\mathcal{R}(\bar{P}^s_{n_-}), \mathcal{R}(Q^u)) > \sigma, \quad \measuredangle(\mathcal{R}(\bar{P}^u_{n_+}), \mathcal{R}(Q^s)) > \sigma, \tag{11}$$

with $0 < \sigma \leq \frac{\pi}{2}$ for sufficiently large $-n_-$, n_+. Note that the angle between two subspaces A and B is defined as, see Golub & Van Loan (1996),

$$\measuredangle(A,B) = \theta \in \left[0, \frac{\pi}{2}\right], \quad \text{where} \quad \cos\theta = \max_{u \in A, \|u\|=1} \max_{v \in B, \|v\|=1} u^T v.$$

(2) Computation of the least squares solution of (5) on J.

The question, whether the numerically computed matrix P_N^s is indeed a projector can be answered by calculating $\|(P_N^s)^2 - P_N^s\|$. This projector residual is analyzed in the following proposition with subsequent results for boundary value and least squares approximations.

Proposition 1 *Let u_n^i be an approximation of $\bar{u}_n^i$ on the intervals $J = [n_-, n_+]$, such that*

$$\|u_n^i - \bar{u}_n^i\| \leq C\varepsilon_n(n_\pm), \quad i \in \{1, \ldots, k\}, \quad n \in J$$

and let $P_N^s := \left(u_N^1, \ldots u_N^k\right)$. Then

$$\|(P_N^s)^2 - P_N^s\| \leq \tilde{C}\varepsilon_N(n_\pm),$$

with an $n_\pm$ independent constant $\tilde{C}$.

Proof: Due to (6) the estimate $\|\bar{P}_N^s - P_N^s\| \leq C_1\varepsilon_N(n_\pm)$ holds.

Let $P_N^s = \bar{P}_N^s + R$, $\|R\| \leq C_1\varepsilon_N(n_\pm)$. It follows that

$$\begin{aligned} \|(P_N^s)^2 - P_N^s\| &= \|(\bar{P}_N^s + R)(\bar{P}_N^s + R) - (\bar{P}_N^s + R)\| \\ &= \|\bar{P}_N^s\bar{P}_N^s - \bar{P}_N^s + \bar{P}_N^s R + R\bar{P}_N^s + RR - R\| \\ &= \|\bar{P}_N^s R + R\bar{P}_N^s + RR - R\| \leq \tilde{C}\varepsilon_N(n_\pm). \end{aligned}$$

■

Note that $\|(P_N^s)^2 - P_N^s\|$ is a lower bound for the approximation error, which one can compute without knowing the exact solution. Assuming an exponential dichotomy on $\mathbb{Z}$, we expect this projector residual to be small. The meaning of a "small" residual is formalized in the following theorems, which state error estimates for numerically computed dichotomy projectors.

2.1 Projection boundary conditions

Theorem 2 *Assume **A1** and let $P_N^{s,u}(n_\pm)$ be approximations on $J = [n_-, n_+]$ of the dichotomy projectors $\bar{P}_N^{s,u}$, computed using the approach* (7) *with projection boundary conditions* (9)*. Further assume that the boundary operator is defined with respect to projectors Q^s, Q^u that satisfy* (11) *and*

$$\Phi(N, n_-)\mathcal{R}(Q^u) \cap \Phi(N, n_+)\mathcal{R}(Q^s) = \{0\}. \tag{12}$$

Then

$$P_N^{s,u}(n_\pm)^2 - P_N^{s,u}(n_\pm) = 0 \tag{13}$$

and

$$\|P_N^{s,u}(n_\pm) - \bar{P}_N^{s,u}\| \leq C\left(\mathrm{e}^{-(\alpha_s+\alpha_u)(N-n_-)} + \mathrm{e}^{-(\alpha_s+\alpha_u)(n_+-N)}\right). \tag{14}$$

Proof: Assumption (12) enables the construction of the projector $P_N^s(n_\pm)$ with range $\Phi(N,n_+)\mathcal{R}(Q^s)$ and nullspace $\Phi(N,n_-)\mathcal{R}(Q^u)$. Define $P_N^u(n_\pm) := I - P_N^s(n_\pm)$ and $P_n^{s,u}(n_\pm) := \Phi(n,N)P_N^{s,u}(n_\pm)\Phi(N,n)$ for $n \in J$, then the cocycle property (42) is satisfied.

The boundary condition (9) requires

$$u_{n_+} \in \mathcal{R}(Q^s) = \Phi(n_+,N)\Phi(N,n_+)\mathcal{R}(Q^s) = \Phi(n_+,N)\mathcal{R}(P_N^s(n_\pm)) = \mathcal{R}(P_{n_+}^s(n_\pm))$$

and similarly $u_{n_-} \in \mathcal{R}(P_{n_-}^u(n_\pm))$. Therefore, the solution of the boundary value problem is given explicitly, using Green's function

$$u_n = G(n,N)r, \quad n \in J, \quad G(n,N) = \begin{cases} \Phi(n,N)P_N^s(n_\pm), & \text{for } n_+ \geq n \geq N, \\ -\Phi(n,N)P_N^u(n_\pm), & \text{for } n_- \leq n < N, \end{cases}$$

in particular $u_N = P_N^s(n_\pm)r$. With $r = e_i$, $i = 1,\ldots,k$, we get the columns of the projector $P_N^s(n_\pm)$ and consequently (13) holds.

Applying (Hüls 2009, Proposition 4), we obtain the estimate

$$\|\bar{u}_N - u_N\| \leq \tilde{C}\left(\mathrm{e}^{-(\alpha_s+\alpha_u)(N-n_-)} + \mathrm{e}^{-(\alpha_s+\alpha_u)(n_+-N)}\right)$$

from which (14) follows.

■

Note that (13) also holds, if the rank of the reference projectors Q^u and Q^s do not equal the rank of the dichotomy projectors. Since the boundary value problem considers only finite intervals, equation (13) is even satisfied, if (4) possesses no exponential dichotomy on $\mathbb{Z}$.

2.2 Periodic boundary conditions

Errors that occur when solving (7) with generalized periodic boundary conditions

$$b(u_{n_-}, u_{n_+}) = u_{n_-} - u_{n_+} - x, \quad x \in \mathbb{R}^k \text{ fixed} \tag{15}$$

are discussed in the following theorem.

Theorem 3 *Assume **A1** and the angle condition* (10)*. Denote by $\bar{u}_\mathbb{Z}$ the unique bounded solution of*

$$u_{n+1} = A_n u_n + \delta_{n,N-1} r, \quad n \in \mathbb{Z}.$$

Then the boundary value problem (7) *with boundary operator* (15) *has a unique solution u_J fulfilling for $n \in J = [n_-, n_+]$:*

$$\|\bar{u}_n - u_n\| \leq C\left(\mathrm{e}^{-\alpha_u(n_+-n)} + \mathrm{e}^{-\alpha_s(n-n_-)}\right)\left(\left(\mathrm{e}^{-\alpha_u(N-n_-)} + \mathrm{e}^{-\alpha_s(n_+-N)}\right)\|r\| + \|x\|\right). \tag{16}$$

Proof: First, we note that the angle conditions (10) guarantees that $\Phi(n_+, n_-)$ has not an eigenvalue 1 for $-n_-, n_+$ sufficiently large. Thus, the periodic boundary value problem has a unique solution, cf. Theorem 8, (a).

Using Green's function, the general solution of the inhomogeneous equation (7) has the form

$$u_n = G(n, N)r + \Phi(n, n_-)v_- + \Phi(n, n_+)v_+, \quad v_- \in \mathcal{R}(\bar{P}^s_{n_-}),\ v_+ \in \mathcal{R}(\bar{P}^u_{n_+}).$$

We choose v_-, v_+ such that the boundary condition is satisfied:

$$\begin{aligned} 0 = u_{n_-} - u_{n_+} - x &= G(n_-, N)r + \Phi(n_-, n_-)v_- + \Phi(n_-, n_+)v_+ \\ &\quad -G(n_+, N)r - \Phi(n_+, n_-)v_- - \Phi(n_+, n_+)v_+ - x. \end{aligned}$$

Thus

$$v_- - v_+ + \Phi(n_-, n_+)v_+ - \Phi(n_+, n_-)v_- = -G(n_-, N)r + G(n_+, N)r + x. \tag{17}$$

Since $\|\Phi(n_+, n_-)v_- + \Phi(n_-, n_+)v_+\|$ converges to 0 exponentially fast, we obtain a unique solution v_-, v_+ of (17) with

$$\begin{aligned} \|v_- - v_+\| &\le \tilde{C}\big(\|G(n_-, N)\| + \|G(n_+, N)\|\big)\|r\| + \|x\| \\ &\le \tilde{C}\big(\|\Phi(n_-, N)\bar{P}^u_N\| + \|\Phi(n_+, N)\bar{P}^s_N\|\big)\|r\| + \|x\| \\ &\le \tilde{C}K\left(\mathrm{e}^{-\alpha_u(N-n_-)} + \mathrm{e}^{-\alpha_s(n_+-N)}\right)\|r\| + \|x\|. \end{aligned}$$

Let $W_{n_\pm}$ be the projector, satisfying $\mathcal{R}(W_{n_\pm}) = \mathcal{R}(\bar{P}^s_{n_-})$, $\mathcal{N}(W_{n_\pm}) = \mathcal{R}(\bar{P}^u_{n_+})$. Using the angle condition (10), we get a uniform upper bound ω for $\|W_{n_\pm}\|$, cf. (Hüls 2009, Lemma A.2) and therefore

$$\begin{aligned} \|v_-\| &= \|W_{n_\pm}(v_- - v_+)\| \le \|W_{n_\pm}\|\|(v_- - v_+)\| \\ &\le \omega\tilde{C}K\left(\mathrm{e}^{-\alpha_u(N-n_-)} + \mathrm{e}^{-\alpha_s(n_+-N)}\right)\|r\| + \|x\|. \end{aligned}$$

Applying the projector $I - W_{n_\pm}$, we prove the same estimate for $\|v_+\|$. As a consequence it holds for $n \in J$ with a constant $C > 0$

$$\begin{aligned} \|\bar{u}_n - u_n\| &= \|\Phi(n, n_+)v_+ + \Phi(n, n_-)v_-\| \\ &\le K\mathrm{e}^{-\alpha_u(n_+-n)}\|v_+\| + K\mathrm{e}^{-\alpha_s(n-n_-)}\|v_-\| \\ &\le C\left(\mathrm{e}^{-\alpha_u(n_+-n)} + \mathrm{e}^{-\alpha_s(n-n_-)}\right)\left(\left(\mathrm{e}^{-\alpha_u(N-n_-)} + \mathrm{e}^{-\alpha_s(n_+-N)}\right)\|r\| + \|x\|\right). \end{aligned}$$

■

When computing dichotomy projectors, using periodic boundary conditions (8), we apply (15) with $x = 0$ and get from Proposition 1 and (16) with $n = N$

$$\begin{aligned} \|P_N(n_\pm)^2 - P_N(n_\pm)\| &\le \bar{C}\left(\mathrm{e}^{-\alpha_u(n_+-N)} + \mathrm{e}^{-\alpha_s(N-n_-)}\right) \\ &\quad \cdot \left(\mathrm{e}^{-\alpha_u(N-n_-)} + \mathrm{e}^{-\alpha_s(n_+-N)}\right)\|r\|. \end{aligned}$$

2.3 Least squares approach

We develop a pointwise estimate by combining Theorem 3 with a uniform estimate from Hüls (2009) of the least squares solution on J.

Theorem 4 *Assume* ***A1****, the angle condition* (10)*, and denote by* $\bar{u}_{\mathbb{Z}}$ *the unique bounded solution of* (5)*.*

Then the least squares solution v_J *of* (7) *satisfies the following inequality:*

$$\begin{aligned} \|\bar{u}_n - v_n\| \;&\leq\; C\|r\| \left(\mathrm{e}^{-\alpha_u(n_+-n)} + \mathrm{e}^{-\alpha_s(n-n_-)}\right) \\ &\quad \cdot (n_+ - n_-)^{\frac{1}{2}} \left(\mathrm{e}^{-\alpha(N-n_-)} + \mathrm{e}^{-\alpha(n_+-N)}\right), \end{aligned} \tag{18}$$

where $\alpha = \min\{\alpha_s, \alpha_u\}$.

Proof: From (Hüls 2009, Theorem 4.1) we obtain that equation (7) has a unique least squares solution v_J, fulfilling the error estimate

$$\sup_{n\in J} \|\bar{u}_n - v_n\| \leq C\|r\|(n_+ - n_-)^{\frac{1}{2}} \left(\mathrm{e}^{-\alpha(N-n_-)} + \mathrm{e}^{-\alpha(n_+-N)}\right). \tag{19}$$

Note that (Hüls 2009, Theorem 4.1) gives an estimate at $N = 0$ with factor $(n_+ - n_-)$ instead of $(n_+ - n_-)^{\frac{1}{2}}$. But a simple inspection of the proof leads to the improved result (19).

For getting a point-wise estimate, we consider the boundary value problem (7) with boundary operator

$$b(u_{n_-}, u_{n_+}) = u_{n_-} - u_{n_+} - x, \qquad \text{where } x = v_{n_-} - v_{n_+}.$$

By Theorem 3, this boundary value problem has a unique solution u_J that therefore coincides with the least squares solution v_J.

Thus $\|\bar{u}_n - v_n\|$ satisfies the inequality (16) with

$$\begin{aligned} \|x\| \;&=\; \|v_{n_-} - v_{n_+}\| \leq \|v_{n_-} - \bar{u}_{n_-}\| + \|\bar{u}_{n_-}\| + \|\bar{u}_{n_+}\| + \|\bar{u}_{n_+} - v_{n_+}\| \\ &\leq\; C\|r\|(n_+ - n_-)^{\frac{1}{2}} \left(\mathrm{e}^{-\alpha(N-n_-)} + \mathrm{e}^{-\alpha(n_+-N)}\right) \\ &\quad + K\mathrm{e}^{-\alpha_u(N-n_-)}\|r\| + K\mathrm{e}^{-\alpha_s(n_+-N)}\|r\|. \end{aligned}$$

This gives the estimate (18) with a generic constant $C > 0$.

■

The corresponding estimate for dichotomy projectors, computed via the least squares approach, follows from (18) with $n = N$.

3 Sacker-Sell spectrum

The Sacker-Sell spectrum, cf. Sacker & Sell (1978), Aulbach & Siegmund (2001), Dieci & Van Vleck (2007), also called dichotomy spectrum is for discrete time dynamical systems defined as

$$\sigma_{\mathrm{ED}} = \{\gamma \in \mathbb{R}^+ : (20) \text{ possesses no exponential dichotomy on } \mathbb{Z}\},$$

where

$$u_{n+1} = \frac{1}{\gamma} A_n u_n, \quad n \in \mathbb{Z}, \tag{20}$$

and the resolvent set is $\mathbb{R}^+ \setminus \sigma_{\mathrm{ED}}$. It is well known that the Sacker-Sell spectrum consists of at most k disjoint, closed intervals, where k denotes the dimension of the space, cf. Sacker & Sell (1978).

The following characterization of exponential dichotomies, see (Palmer 1988, Proposition 2.6) gives in case of half-sided dichotomies a criterion for analyzing whether γ lies in the spectrum or in the resolvent set.

Proposition 5 *The following statements are equivalent:*

- *The difference equation* (4) *possesses an exponential dichotomy on* $\mathbb{Z}$.
- (4) *has exponential dichotomies on* $\mathbb{Z}^-$ *and* $\mathbb{Z}^+$ *with projectors of equal rank, and* (4) *has no bounded, non-trivial solution on* $\mathbb{Z}$.

Denote by $\Phi(n, m)$ the solution operator of (4). Then the solution operator of the scaled equation (20) is

$$\Phi_\gamma(n, m) = \gamma^{m-n} \Phi(n, m).$$

Let L be an interval in the resolvent set, i.e. $L \cap \sigma_{\mathrm{ED}} = \emptyset$. For $\gamma \in L$ one has

$$\|\Phi_\gamma(n, m) P_m^s\| = \gamma^{m-n} \|\Phi(n, m) P_m^s\| \leq K \mathrm{e}^{-\alpha_s (n-m)} \gamma^{m-n} = K \mathrm{e}^{-(\alpha_s + \ln \gamma)(n-m)},$$

and similarly, the corresponding estimate in the unstable direction follows. Thus, the scaled equation possesses in the resolvent-interval containing 1, the same dichotomy projectors as the original equation (4). Furthermore, the dichotomy projectors as well as the constant K are in a resolvent-interval independent of γ.

Example 6 *The difference equation*

$$u_{n+1} = A_n u_n, \quad \text{where } A_n = \begin{cases} A_-, & \text{for } n \leq 0, \\ A_+, & \text{for } n \geq 1, \end{cases}$$

with

$$A_- = \begin{pmatrix} 1 & & \\ & 4 & \\ & & 6 \end{pmatrix} \quad \text{and} \quad A_+ = \begin{pmatrix} 2 & & \\ & 3 & \\ & & 5 \end{pmatrix} \tag{21}$$

possesses an exponential dichotomy on $\mathbb{Z}^-$ *for* $\gamma \notin \{1, 4, 6\}$ *and on* $\mathbb{Z}^+$ *for* $\gamma \notin \{2, 3, 5\}$. *Due to Proposition 5, these dichotomies cannot be extended to* $\mathbb{Z}$ *for values of* γ *from the union of intervals* $\sigma := [1, 2] \cup [3, 4] \cup [5, 6]$.

We transform this equation into a more general form: Let S_1 *and* S_2 *be two non-singular matrices and define the difference equation*

$$u_{n+1} = A_n u_n, \quad \text{where } A_n = \begin{cases} S_1 A_- S_1^{-1}, & \text{for } n \leq 0, \\ S_2 A_+ S_2^{-1}, & \text{for } n \geq 1, \end{cases} \tag{22}$$

with matrices $A_\pm$ from (21). *Denote by $P_n^{-s,-u}(\gamma)$ and $P_n^{+s,+u}(\gamma)$ the corresponding half-sided dichotomy projectors of the scaled equation* (20) *on $\mathbb{Z}^-$ and $\mathbb{Z}^+$. By Proposition 5, these dichotomies can be combined to a dichotomy on $\mathbb{Z}$, if no bounded, non-trivial solution exists. Thus*

$$\sigma_{ED} = \sigma \quad \text{if} \quad \mathcal{R}(P_0^{-u}(\gamma)) \cap \mathcal{R}(P_0^{+s}(\gamma)) = \{0\} \text{ for } \gamma \notin \sigma. \tag{23}$$

For $\gamma \in (2,3)$, the half-sided dichotomy projectors are

$$P_0^{-u}(\gamma) = S_1 \begin{pmatrix} 0 & & \\ & 1 & \\ & & 1 \end{pmatrix} S_1^{-1}, \quad P_0^{+s}(\gamma) = S_2 \begin{pmatrix} 1 & & \\ & 0 & \\ & & 0 \end{pmatrix} S_2^{-1}$$

and for $\gamma \in (4,5)$ we obtain

$$P_0^{-u}(\gamma) = S_1 \begin{pmatrix} 0 & & \\ & 0 & \\ & & 1 \end{pmatrix} S_1^{-1}, \quad P_0^{+s}(\gamma) = S_2 \begin{pmatrix} 1 & & \\ & 1 & \\ & & 0 \end{pmatrix} S_2^{-1}.$$

Thus (23) *is equivalent to non-singularity of the matrices $\begin{pmatrix} S_1e_2 & S_1e_3 & S_2e_1 \end{pmatrix}$ and $\begin{pmatrix} S_1e_3 & S_2e_1 & S_2e_2 \end{pmatrix}$.*

We introduce three tests for detecting Sacker-Sell spectral intervals. In a given interval L, we choose a grid L_g and compute for each $\gamma \in L_\mathrm{g}$ a quantity that indicates whether (20) has an exponential dichotomy. The first test is based on computing dichotomy projectors, while the second and third one analyze solutions of boundary value problems at end- or midpoints.

3.1 Numerical detection of Sacker-Sell spectral intervals via dichotomy projectors

From Theorem 3 and 4 we know that if an exponential dichotomy exists, then the projector residual $\|P^2 - P\|$ is small, i.e. (14) and (18) hold in case of periodic boundary- and least squares-computations, respectively. But if the projector residual does not satisfy the corresponding inequality, then the difference equation cannot have an exponential dichotomy on $\mathbb{Z}$.

As a toy model, we choose the difference equation from Example 6. We compute for equidistantly chosen values $\gamma \in [0.01, 10]$ the dichotomy projector $P_N^s(\gamma)$ and plot $\|P_N^s(\gamma)^2 - P_N^s(\gamma)\|$. For these calculations, the periodic boundary value ansatz or alternatively the least squares approach is applied. Note that this test is not working with projection boundary conditions, since these boundary conditions always give exact projectors, cf. Theorem 2.

When discussing the costs of boundary value and least squares approach, one sees that the boundary value approach requires to solve k linear systems (7) with unit vectors as right hand side.

The least squares solution of this problem is given as $u_J = B^+ R$, where $B^+ = B^T(BB^T)^{-1}$ and

$$B = \begin{pmatrix} -A_{n_-} & I & & \\ & \ddots & \ddots & \\ & & -A_{n_+-1} & I \end{pmatrix}, \quad u_J = \begin{pmatrix} u_{n_-} \\ \vdots \\ u_{n_+} \end{pmatrix}, \quad R_i = \begin{cases} 0, & i \in J,\ i \neq N-1, \\ I, & i = N-1, \end{cases}$$

cf. Hüls (2009). For the computation of the Moore-Penrose inverse, we refer to Shinozaki et al. (1972). The dichotomy projector is the N-th block component of the solution u_J. As a consequence, the Moore-Penrose inverse contains approximations of all dichotomy projectors within the finite interval. More precisely, the n-th block-row of the $(n-1)$-th block-column of B^+ is an approximation of the dichotomy projector $\bar{P}^s_{n+n_--1}$.

For computing the matrix B^+_{ij}, containing the columns from i to j of B^+, we numerically solve

$$BB^t w = [e_i \dots e_j] \tag{24}$$

with a sparse LU-decomposition and obtain

$$B^+_{ij} = B^T w. \tag{25}$$

Also the boundary value solution is computed, using a sparse LU-decomposition.

The resulting techniques are applied to the example (22) for $\pm n_\pm \in \{100, 1000\}$ and $N = 0$. In the least squares approach, we simultaneously compute 100 dichotomy projectors by solving (24) and (25) for $i = (-n_- - 50)k + 1$ and $j = (-n_- + 50)k$, where $k = 3$ is the dimension of the space. A plot of the projector residual over γ is given in Figure 1.

For periodic boundary value computations, we observe in Figure 1 that the projector residual is small in the resolvent set, as suggested by (14). But also in the shaded spectral intervals, this residual is of order Δ, except for a peak around the midpoint of each interval that becomes more and more narrow as $\pm n_\pm \to \infty$. Here Δ denotes the machine accuracy. A closer inspection of the resulting projector P for $\gamma = 3.3$ and $\pm n_\pm = 1000$ reveals that

$$P = S_2 \begin{pmatrix} 1 & a & b \\ 0 & 0 & 0 \\ 0 & 0 & 0 \end{pmatrix} S_2^{-1}$$

with some $a, b \in \mathbb{R}$ that depend on the choice of S_1 and S_2.

One the other hand, projector residuals that are computed with the least squares approach satisfy (18) in the resolvent set. Furthermore, Figure 1 illustrates that these residuals are of order 1 in the shaded spectral intervals and therefore detect nicely the Sacker-Sell spectrum. Currently we have no detailed explanation of this behavior in the spectral intervals.

In the following section, we introduce a finer test for the precise detection of the Sacker-Sell spectrum that is based on solving boundary value problems.

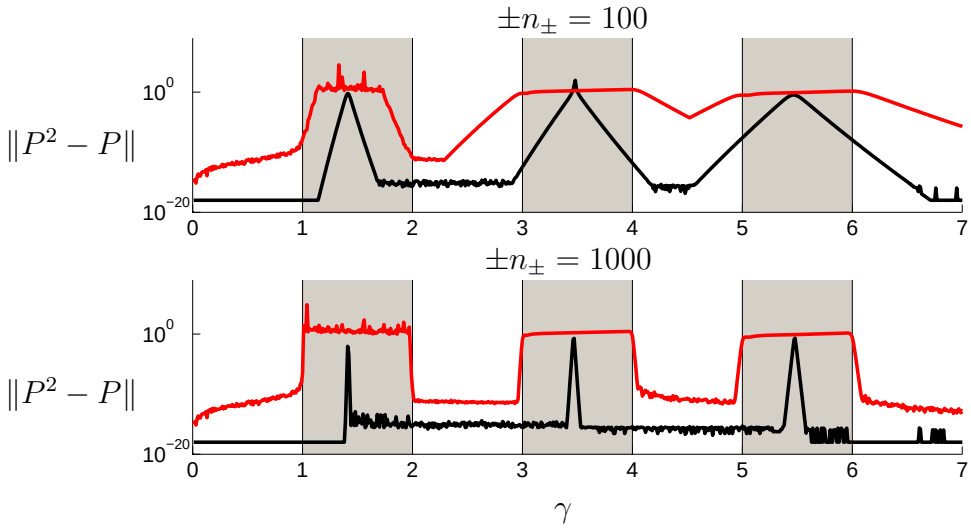

Figure 1: *Detection of Sacker-Sell spectral intervals (marked in gray) for Example 6 via the projector residual for* $\pm n_\pm = 100$ *(upper figure) and* $\pm n_\pm = 1000$ *(lower figure). The red curves are computed with the least squares ansatz, while the black curves use the boundary value approach with periodic boundary conditions.*

3.2 Numerical detection of Sacker-Sell spectral intervals via boundary value solutions

In this section, we consider Sacker-Sell spectral intervals, caused by half-sided dichotomies on $\mathbb{Z}^-$ and $\mathbb{Z}^+$ that cannot be combined to an exponential dichotomy on $\mathbb{Z}$, see Proposition 5. We introduce two dichotomy tests that are based on solving boundary value problems

$$u_{n+1} = A_n u_n + \delta_{n,N-1} r, \quad n = n_-, \dots, n_+ - 1, \tag{26}$$

$$u_{n_-} = u_{n_+} + x. \tag{27}$$

Compared to the method from Section 3.1, this approach is also feasible to high dimensional systems.

Denote by $P_n^{-s,-u}$ and $P_n^{+s,+u}$ half-sided dichotomy projectors on $\mathbb{Z}^-$ and $\mathbb{Z}^+$, respectively. In the resolvent set, one has

$$\operatorname{rank}(P_N^{-u}) + \operatorname{rank}(P_N^{+s}) = k \quad \text{and} \quad \mathcal{R}(P_N^{-u}) \oplus \mathcal{R}(P_N^{+s}) = \mathbb{R}^k,$$

while the following cases may occur in spectral intervals:

(i) $\operatorname{rank}(P_N^{-u}) + \operatorname{rank}(P_N^{+s}) \geq k + 1$. Then, the inhomogeneous equation (26) generically has infinitely many bounded solutions on $\mathbb{Z}$.

(ii) $\operatorname{rank}(P_N^{-u}) + \operatorname{rank}(P_N^{+s}) \le k-1$. In this case (26) generically has no bounded solution on $\mathbb{Z}$.

(iii) $\operatorname{rank}(P_N^{-u}) + \operatorname{rank}(P_N^{+s}) = k$ and $\mathcal{R}(P_N^{-u}) \cap \mathcal{R}(P_N^{+s}) \neq \{0\}$. This situation occurs, for example, when considering the variational equation along a tangential homoclinic orbit.

The first case (i) can be reduced to (ii) and vice versa, by considering the adjoint equation

$$v_{n+1} = (A_{n+1}^{-1})^T v_n, \quad n \in \mathbb{Z}, \tag{28}$$

cf. Palmer (1988). If (4) possesses half-sided dichotomies with data $(K^{\pm}, \alpha_s^{\pm}, \alpha_u^{\pm}, P_n^{\pm s}, P_n^{\pm u})$, then the adjoint equation (28) also has half-sided dichotomies with data $(\tilde{K}^{\pm}, \alpha_u^{\pm}, \alpha_s^{\pm}, (P_{n+1}^{\pm u})^T, (P_{n+1}^{\pm s})^T)$. Obviously, the sets of γ-values coincide, in which the scaled equations

$$u_{n+1} = \frac{1}{\gamma} A_n u_n \quad \text{and} \quad v_{n+1} = \gamma (A_{n+1}^{-1})^T v_n$$

have an exponential dichotomy on $\mathbb{Z}$. If the adjoint equation has infinitely many bounded solutions on $\mathbb{Z}$, then (2) generically has no bounded solution. As a consequence, it suffices to construct a test that distinguishes (ii) and (iii) from the resolvent case. An alternative test that avoids computations with the adjoint equation is discussed at the end of this section.

The norm of the end points u_{n_-} and u_{n_+} is an indicator for detecting spectral intervals. First, we show that in the resolvent set, this expression is bounded from above.

Theorem 7 *Assume* ***A1****, the angle condition* (10) *and denote by* $\bar{u}_{\mathbb{Z}}$ *the unique bounded solution of* (26) *on* $\mathbb{Z}$*. Let* $(u_n)_{n\in[n_-,n_+]}$ *be the solution of the finite boundary value problem* (26), (27)*, with* $\|r\| = \|x\| = 1$*. Then*

$$\|u_n\| \le C \begin{cases} \mathrm{e}^{-\alpha_s(n-N)} + \mathrm{e}^{-\alpha_u(n_+-n)}, & \text{for } n_+ \ge n > N, \\ \mathrm{e}^{-\alpha_u(N-n)} + \mathrm{e}^{-\alpha_s(n-n_-)}, & \text{for } n_- \le n < N. \end{cases}$$

Proof: Let $n_+ \ge n > N$. Applying Theorem 3, we get

$$\begin{aligned} \|u_n\| &\le \|u_n - \bar{u}_n\| + \|\bar{u}_n\| = \|u_n - \bar{u}_n\| + \|\Phi(n,N)P_N^s r\| \\ &\le C\left(\mathrm{e}^{-\alpha_u(n_+-n)} + \mathrm{e}^{-\alpha_s(n-n_-)}\right)\left(\left(\mathrm{e}^{-\alpha_u(N-n_-)} + \mathrm{e}^{-\alpha_s(n_+-N)}\right)\|r\| + \|x\|\right) \\ &\quad + K\mathrm{e}^{-\alpha_s(n-N)}\|r\| \\ &\le \tilde{C}\left(\mathrm{e}^{-\alpha_u(n_+-n)} + \mathrm{e}^{-\alpha_s(n-N)}\right). \end{aligned}$$

Similarly, we obtain for $n_- \le n < N$ the second assertion.

■

Our tests for detecting spectral intervals are based on this estimate. Roughly speaking, the difference equation (4) has no exponential dichotomy on $\mathbb{Z}$, if $\|u_{n_\pm}\|$ is unbounded, cf. case (ii).

An existence result for the solution of the boundary value problem as well as estimates of $\|u_{n_\pm}\|$ in case of half-sided dichotomies are given in the following theorem. Assume

$$\mathbb{R}^k = \mathcal{R}(P_N^{-u}) \oplus \mathcal{R}(P_N^{+s}) \oplus (\mathcal{R}(P_N^{-s}) \cap \mathcal{R}(P_N^{+u})) \tag{29}$$

and note that generic systems, fulfilling (ii) also satisfy this assumption.

Theorem 8 *Let $n_- < N < n_+$ and assume that 1 is not an eigenvalue of $\Phi(n_-, n_+)$.*

(a) Then the boundary value problem (26), (27) has a unique solution.

(b) Further assume that (4) possesses exponential dichotomies on $\mathbb{Z}^-$ and $\mathbb{Z}^+$ with data $(K^\pm, \alpha_s^\pm, \alpha_u^\pm, P_n^{\pm s}, P_n^{\pm u})$, such that

$$\mathbb{R}^k = X \oplus Y,\ X = \mathcal{R}(P_N^{-u}) \oplus \mathcal{R}(P_N^{+s}),\ Y = \mathcal{R}(P_N^{-s}) \cap \mathcal{R}(P_N^{+u}),\ \dim Y \geq 1. \tag{30}$$

Let $r = r_X + r_Y$, $r_X \in X$, $0 \neq r_Y \in Y$ and $n_- \leq n_1 < N < n_2 \leq n_+$. Then

$$\|u_{n_1}\| + \|u_{n_2}\| \geq \|r_Y\| \frac{C}{\mathrm{e}^{-\alpha_s^-(N-n_1)} + \mathrm{e}^{-\alpha_u^+(n_2-N)}}. \tag{31}$$

(c) Assume that (4) has exponential dichotomies on $\mathbb{Z}^-$ and $\mathbb{Z}^+$ such that

$$\operatorname{rank}(P_N^{-u}) + \operatorname{rank}(P_N^{+s}) = k \quad \text{and} \quad \mathcal{R}(P_N^{-u}) \cap \mathcal{R}(P_N^{+s}) \neq \{0\}.$$

Let $\mathbb{R}^k = X \oplus Y$, where $X = \mathcal{R}(P_N^{-u}) + \mathcal{R}(P_N^{+s})$, $Y = X^\perp$, $\dim Y \geq 1$. Then, (31) holds.

Proof:

(a) Two half-sided solutions of the homogeneous equation are

$$\begin{aligned} u_n^- &= \Phi(n, n_-)v_-, \quad \text{for } n \leq N, \\ u_n^+ &= \Phi(n, n_+)v_+, \quad \text{for } n \geq N. \end{aligned}$$

These half-sided solutions form a solution of the inhomogeneous equation, if

$$u_N^+ = A_{N-1}u_{N-1}^- + r \quad \Leftrightarrow \quad \Phi(N, n_+)v_+ = \Phi(N, n_-)v_- + r. \tag{32}$$

Further, the boundary condition (27) requires that $v_- = v_+ + x$.

Therefore, we get

$$\begin{aligned} \Phi(N, n_-)v_+ + \Phi(N, n_-)x + r &= \Phi(N, n_+)v_+ \\ \Leftrightarrow\ (\Phi(N, n_+) - \Phi(N, n_-))v_+ &= \Phi(N, n_-)x + r \\ \Leftrightarrow\ (\Phi(n_-, n_+) - I)v_+ &= x + \Phi(n_-, N)r. \end{aligned}$$

By assumption, $\Phi(n_+, n_-) - I$ is invertible, and we obtain a unique solution v_+, $v_- = v_+ + x$.

(b) Let W be the projector with $\mathcal{R}(W) = Y$, $\mathcal{N}(W) = X$. Using equation (32) it follows that

$$\begin{aligned} r_Y &:= Wr = W\left(-\Phi(N,n_1)u_{n_1} + \Phi(N,n_2)u_{n_2}\right) \\ &= -WP_N^{-s}\Phi(N,n_1)u_{n_1} + WP_N^{+u}\Phi(N,n_2)u_{n_2} \\ &= W\left(-\Phi(N,n_1)P_{n_1}^{-s}u_{n_1} + \Phi(N,n_2)P_{n_2}^{+u}u_{n_2}\right). \end{aligned}$$

From the half-sided dichotomies, we obtain

$$\begin{aligned} \|r_Y\| &\leq \|W\|\left(\|\Phi(N,n_1)P_{n_1}^{-s}\|\|u_{n_1}\| + \|\Phi(N,n_2)P_{n_2}^{+u}\|\|u_{n_2}\|\right) \\ &\leq \|W\|\left(K^-\mathrm{e}^{-\alpha_s^-(N-n_1)}\|u_{n_1}\| + K^+\mathrm{e}^{-\alpha_u^+(n_2-N)}\|u_{n_2}\|\right) \\ &\leq \tilde{C}\left(\mathrm{e}^{-\alpha_s^-(N-n_1)} + \mathrm{e}^{-\alpha_u^+(n_2-N)}\right)\left(\|u_{n_1}\| + \|u_{n_2}\|\right) \end{aligned}$$

which proves (31).

(c) The proof of the tangential case follows along the lines of part (b), but with the settings $X = \mathcal{R}(P_N^{-u}) + \mathcal{R}(P_N^{+s})$, $Y = X^\perp$.

■

If the difference equation possesses for all $\gamma \in \sigma_{\mathrm{ED}}^\circ$ half-sided dichotomies with stable projectors of different rank, then either the original or the adjoint equation generically meets assumption (30) from Theorem 8 and consequently, the corresponding solution exhibits exponential growth towards the end points. This exponential growth enables the numerical detection of Sacker-Sell spectral intervals. Note that the half-sided dichotomy rates also depend on γ. At the boundary of a spectral interval α_s^- or α_u^+ is zero, while these quantities increase towards the midpoint of the spectral interval.

For Example 6, Figure 2 shows $\|u_{n_-}(\gamma)\| + \|u_{n_+}(\gamma)\|$ for the original and for the adjoint equation. We solve the boundary value problem, using a sparse LU-decomposition, for $n_- = -100$, $n_+ = 100$, $N = 0$ and for two random vectors x, r, normalized to length 1. Particularly, one can read off from Figure 2 the type of one-sided dichotomies that lead to spectral intervals. In the interval $[1, 2]$, an increase in the norm of the end points for the original equation corresponds to case (ii), while the remaining spectral intervals are of type (i).

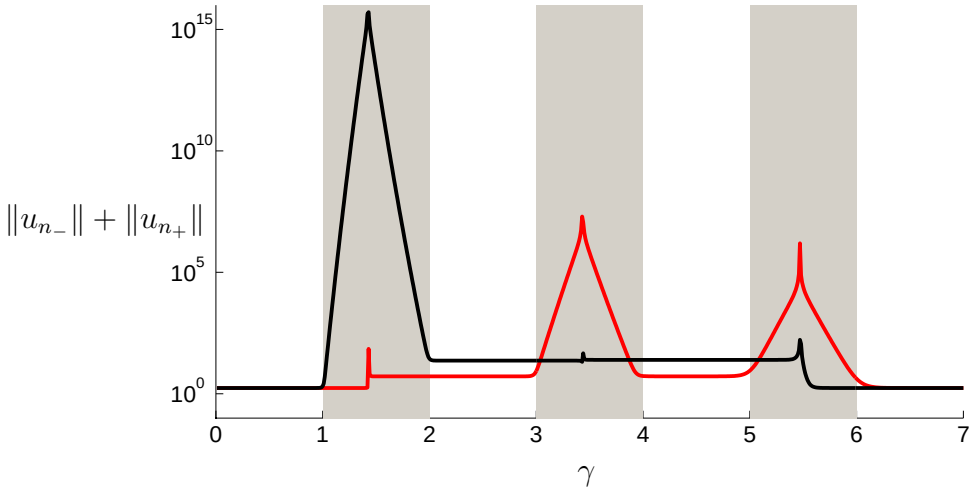

Figure 2: *Detection of Sacker-Sell spectral intervals (marked in gray) for Example 6. The black curve is computed for the original equation, while the red curve shows the result for the adjoint equation.*

In case $\operatorname{rank}(P_N^{-u}) + \operatorname{rank}(P_N^{+s}) \geq k+1$ it is possible to detect spectral intervals directly, by working with the original equation, instead, as suggested before, by using the adjoint equation. We show that the solution of the boundary value problem (26), (27) increases exponentially fast toward the midpoint N.

Theorem 9 *Let $n_- \leq n_1 < N < n_2 \leq n_+$ and assume that 1 is not an eigenvalue of $\Phi(n_-, n_+)$. Further assume that (4) possesses exponential dichotomies on $\mathbb{Z}^-$ and $\mathbb{Z}^+$ with data $(K^{\pm}, \alpha_s^{\pm}, \alpha_u^{\pm}, P_n^{\pm s}, P_n^{\pm u})$, such that $\mathbb{R}^k = X_{n_\pm} \oplus Y_{n_\pm}$, $X_{n_\pm} = \mathcal{R}(P_{n_-}^{-s}) + \mathcal{R}(P_{n_+}^{+u})$, $Y_{n_\pm} = X_{n_\pm}^{\perp}$, $\dim Y_{n_\pm} \geq 1$.*

Let $W_{n_\pm}$ be the projector with $\mathcal{R}(W_{n_\pm}) = Y_{n_\pm}$ and $\mathcal{N}(W_{n_\pm}) = X_{n_\pm}$. Then the solution of (26), (27) satisfies

$$\|u_{n_1}\| + \|u_{n_2}\| \geq \|W_{n_\pm} x\| \frac{C}{\mathrm{e}^{-\alpha_u^-(n_1 - n_-)} + \mathrm{e}^{-\alpha_s^+(n_+ - n_2)}}. \tag{33}$$

Note that $\|W_{n_\pm} x\|$ depends, due to the construction of $X_{n_\pm}$ and $Y_{n_\pm}$, on $n_\pm$. Nevertheless, one can neglect this influence in numerical computations, if the vector x is chosen in a generic position.

Proof: Denote by $(u_n)_{n\in[n_-,n_+]}$ the solution of (26). Then the boundary condition (27) has the form

$$u_{n_-} - u_{n_+} = \Phi(n_-, n_1)u_{n_1} - \Phi(n_+, n_2)u_{n_2} = x.$$

Thus, we get

$$\begin{aligned} W_{n_\pm} x &= W_{n_\pm}\big(\Phi(n_-, n_1)u_{n_1} - \Phi(n_+, n_2)u_{n_2}\big) \\ &= W_{n_\pm}\big(P_{n_-}^{-u}\Phi(n_-, n_1)u_{n_1} - P_{n_+}^{+s}\Phi(n_+, n_2)u_{n_2}\big) \end{aligned}$$

and consequently

$$\begin{aligned}\|W_{n_\pm}x\| &\leq \|W_{n_\pm}\|\big(\|\Phi(n_-,n_1)P_{n_1}^{-u}\| + \|\Phi(n_+,n_2)P_{n_2}^{+s}\|\big)(\|u_{n_1}\| + \|u_{n_2}\|)\\ &\leq C\left(\mathrm{e}^{-\alpha_u^-(n_1-n_-)} + \mathrm{e}^{-\alpha_s^+(n_+-n_2)}\right)(\|u_{n_1}\| + \|u_{n_2}\|),\end{aligned}$$

which proves (33). ■

We apply this idea to Example 6, and choose $n_- = -100$, $n_+ = 100$, $n_1 = -50$, $n_2 = 50$, x and r are, as before, random vectors of length 1. A plot of $\|u_{n_1}(\gamma)\|$ and $\|u_{n_2}(\gamma)\|$ over γ is shown in Figure 3.

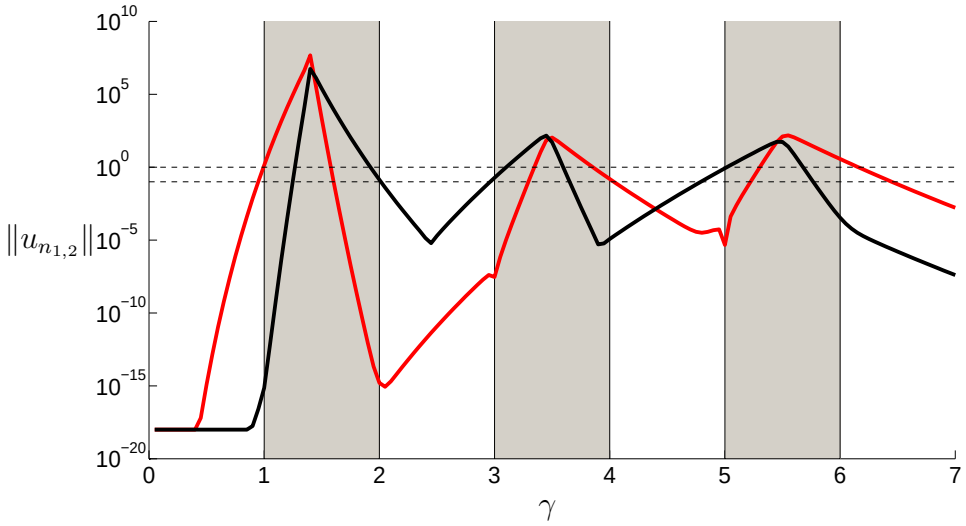

Figure 3: *Detection of Sacker-Sell spectral intervals (marked in gray) for Example 6;* $\|u_{n_1}(\gamma)\|$ *in red and* $\|u_{n_2}(\gamma)\|$ *in black. The dashed lines are placed at* 1 *and* 0.1.

Figure 4 shows the results for the tangential case (iii). In contrast to the previous computations, we change S_2e_1 to S_1e_2 in Example 6 and consequently, $\begin{pmatrix}S_1e_2 & S_1e_3 & S_2e_1\end{pmatrix}$ is singular, while $\begin{pmatrix}S_1e_3 & S_2e_1 & S_2e_2\end{pmatrix}$ is regular. It can clearly be observed that the interval $[2,3]$ belongs to the spectral set, cf. Theorem 8, (c).

3.3 Convergence of approximate spectral intervals

Let n_1 and n_2 be the midpoints of the respective half-intervals

$$n_1 = \left\lfloor \frac{n_- + N}{2} \right\rfloor, \quad \text{and} \quad n_2 = \left\lfloor \frac{n_+ + N}{2} \right\rfloor.$$

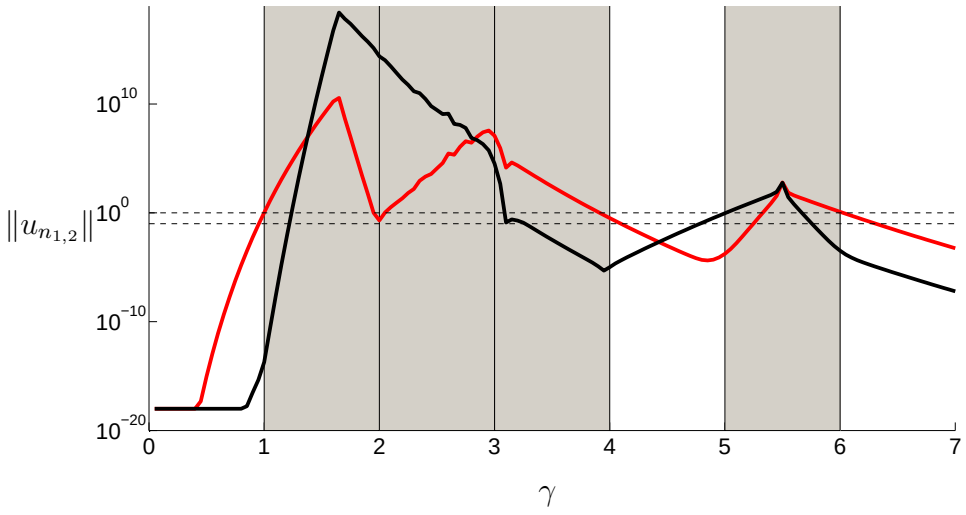

Figure 4: *Detection of Sacker-Sell spectral intervals (marked in gray) for Example 6 in a tangential case;* $\|u_{n_1}(\gamma)\|$ *in red and* $\|u_{n_2}(\gamma)\|$ *in black. The dashed lines are placed at* 1 *and* 0.1.

If the original equation (4) has an exponential dichotomy with rates α_s, α_u, then the scaled equation (20) has the dichotomy rates $\alpha_s + \ln\gamma$ and $\alpha_u - \ln\gamma$ for $|\gamma - 1|$ sufficiently small.

In spectral intervals, we get under the assumptions of Theorem 8

$$\|u_{n_1}(\gamma)\| + \|u_{n_2}(\gamma)\| \geq \|r_Y\| \frac{C}{\mathrm{e}^{-(\alpha_s^- + \ln\gamma)\left(\frac{N-n_-}{2}\right)} + \mathrm{e}^{-(\alpha_u^+ - \ln\gamma)\left(\frac{n_+ - N}{2}\right)}},$$

and in case of Theorem 9, we obtain

$$\|u_{n_1}(\gamma)\| + \|u_{n_2}(\gamma)\| \geq \|W_{n_\pm} x\| \frac{C}{\mathrm{e}^{-(\alpha_u^- - \ln\gamma)\left(\frac{N-n_-}{2}\right)} + \mathrm{e}^{-(\alpha_s^+ + \ln\gamma)\left(\frac{n_+ - N}{2}\right)}}.$$

We assume a uniform lower bound for $\|r_Y\|$ and $\|W_{n_\pm} x\|$ which is typically satisfied in our numerical computations, where r and x are chosen at random.

In the resolvent set, it follows from Theorem 7

$$\|u_{n_1}(\gamma)\| \leq C_1 \left(\mathrm{e}^{-(\alpha_u - \ln\gamma)\left(\frac{N-n_-}{2}\right)} + \mathrm{e}^{-(\alpha_s + \ln\gamma)\left(\frac{N-n_-}{2}\right)} \right), \tag{34}$$

$$\|u_{n_2}(\gamma)\| \leq C_2 \left(\mathrm{e}^{-(\alpha_s + \ln\gamma)\left(\frac{n_+ - N}{2}\right)} + \mathrm{e}^{-(\alpha_u - \ln\gamma)\left(\frac{n_+ - N}{2}\right)} \right). \tag{35}$$

Consequently, if the solution $u_{\mathbb{Z}}(\gamma)$ of the inhomogeneous scaled equation (2) satisfies

$$\max\{\|u_{n_1}(\gamma)\|, \|u_{n_2}(\gamma)\|\} \leq \varepsilon \tag{36}$$

for $-n_-$, n_+ sufficiently large and ε small, then our results guarantee that γ lies in the resolvent set.

In particular

$$\bar{\gamma}_- = \mathrm{e}^{-\alpha_s}, \quad \bar{\gamma}_+ = \mathrm{e}^{\alpha_u}$$

defines the boundary of a resolvent interval. Using (36), we get the numerically computed boundaries

$$\gamma_-^{\mathrm{num}} = \min_{\gamma\in[\bar{\gamma}_-,\bar{\gamma}_+]} \big\{ \max\{\|u_{n_1}(\gamma)\|, \|u_{n_2}(\gamma)\|\} \le \varepsilon\big\}, \tag{37}$$

$$\gamma_+^{\mathrm{num}} = \max_{\gamma\in[\bar{\gamma}_-,\bar{\gamma}_+]} \big\{ \max\{\|u_{n_1}(\gamma)\|, \|u_{n_2}(\gamma)\|\} \le \varepsilon\big\}. \tag{38}$$

Theorem 10 *With the notions and assumptions from above, it holds for $-n_-$, n_+ sufficiently large that*

$$\bar{\gamma}_- \le \gamma_-^{\mathrm{num}} \le \bar{\gamma}_- \cdot \max\left\{ \mathrm{e}^{-\ln\left(\frac{\varepsilon}{C_1}\right)\frac{2}{N-n_-}}, \mathrm{e}^{-\ln\left(\frac{\varepsilon}{C_2}\right)\frac{2}{n_+-N}} \right\},$$

$$\bar{\gamma}_+ \ge \gamma_+^{\mathrm{num}} \ge \bar{\gamma}_+ \cdot \min\left\{ \mathrm{e}^{\ln\left(\frac{\varepsilon}{C_1}\right)\frac{2}{N-n_-}}, \mathrm{e}^{\ln\left(\frac{\varepsilon}{C_2}\right)\frac{2}{n_+-N}} \right\}.$$

Proof: Applying (34), (35) for γ_-^{num} close to $\bar{\gamma}_- = \mathrm{e}^{-\alpha_s}$ yields

$$\varepsilon \le \|u_{n_1}(\gamma_-^{\mathrm{num}})\| \le C_1 \mathrm{e}^{-(\alpha_s+\ln\gamma_-^{\mathrm{num}})\frac{N-n_-}{2}}, \tag{39}$$

$$\varepsilon \le \|u_{n_2}(\gamma_-^{\mathrm{num}})\| \le C_2 \mathrm{e}^{-(\alpha_s+\ln\gamma_-^{\mathrm{num}})\frac{n_+-N}{2}}, \tag{40}$$

and consequently we obtain from (39) that $\gamma_-^{\mathrm{num}} \le \mathrm{e}^{-\ln\left(\frac{\varepsilon}{C_1}\right)\frac{2}{N-n_-}}\mathrm{e}^{-\alpha_s}$ and from (40) we get $\gamma_-^{\mathrm{num}} \le \mathrm{e}^{-\ln\left(\frac{\varepsilon}{C_2}\right)\frac{2}{n_+-N}}\mathrm{e}^{-\alpha_s}$.

Combining these two results, the first estimate follows. Similarly, we prove the second estimate for γ_+^{num} close to $\bar{\gamma}_+ = \mathrm{e}^{\alpha_u}$.

■

We use (37) and (38) numerically and obtain $\gamma_\pm^{\mathrm{num}}$ for Example 6 with $\varepsilon = 0.1$ and $-n_-, n_+ \in \{100, 500, 2000\}$, cf. Table 1. The solutions of the respective boundary value problems are computed for $\gamma = 0.01 \cdot i$, $i = 1, \ldots, 700$.

$\pm n_\pm$			
100	[0.90, 2.13]	[2.85, 4.20]	[4.80, 6.78]
500	[0.99, 2.01]	[2.96, 4.05]	[4.97, 6.14]
2000	[1.00, 2.00]	[2.99, 4.01]	[4.99, 6.04]

Table 1: *Computation of spectral intervals.*

4 Sacker-Sell spectrum along Hénon orbits

We apply the algorithms from the previous section to the variational equation along orbits of the well known Hénon map, cf. Hénon (1976), Mira (1987), Devaney (1989), Hale & Koçak (1991), defined as

$$f(x) = \begin{pmatrix} 1 + x_2 - a x_1^2 \\ b x_1 \end{pmatrix} \qquad \text{with parameters} \qquad a = 1.4,\ b = 0.4.$$

4.1 Heteroclinic orbits

First, a heteroclinic orbit

$$\bar{x}_{n+1} = f(\bar{x}_n),\ n \in \mathbb{Z}, \quad \lim_{n \to \pm\infty} \bar{x}_n = \xi_\pm$$

with respect to the fixed points

$$\xi_\pm = \begin{pmatrix} z \\ bz \end{pmatrix} \quad \text{where} \quad z = \frac{b - 1 \mp \sqrt{(b-1)^2 + 4a}}{2a}$$

is computed, using the techniques, introduced in Beyn et al. (2004), Hüls (2005).

Note that an exponential dichotomy on $\mathbb{Z}$ of the variational equation

$$u_{n+1} = Df(\bar{x}_n) u_n, \quad n \in \mathbb{Z},$$

is equivalent to transversal intersections of the unstable manifold of ξ_- with the stable manifold of ξ_+. The Sacker-Sell spectrum and especially its distance from 1 gives information about the closeness to tangential heteroclinic orbits. The results of the algorithms from the previous section for $\pm n_\pm = 100$ are given in Figures 5, 6 and Table 2.

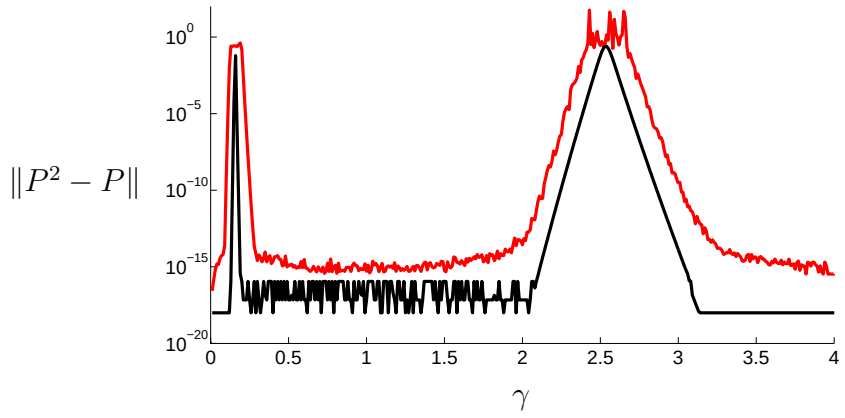

Figure 5: *Detection of Sacker-Sell spectral intervals for the variational equation along a heteroclinic Hénon orbit. Projector residual of the least squares ansatz in red and of the boundary value approach in black.*

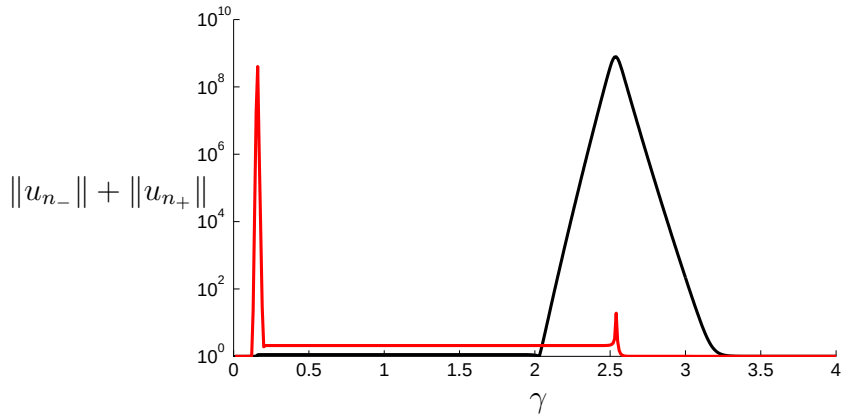

Figure 6: *Detection of Sacker-Sell spectral intervals for the variational equation along a heteroclinic Hénon orbit, via the second approach, applied to the original equation (black) and the adjoint equation (red).*

$\pm n_\pm$		
100	[0.122, 0.205]	[1.999, 3.275]
500	[0.126, 0.198]	[2.030, 3.188]
2000	[0.127, 0.196]	[2.036, 3.172]

Table 2: *Computation of spectral intervals along a heteroclinic orbit with a sampling of* γ *in* 0.001 *steps and* $\varepsilon = 0.1$*, using the midpoints* $u_{n_{1,2}}$.

Note that $Df(\xi_-)$ possesses the eigenvalues $\sigma_1 \approx -2.0376$ and $\sigma_2 \approx 0.1963$ while the eigenvalues of $Df(\xi_+)$ are $\sigma_3 \approx 3.1676$ and $\sigma_4 \approx -0.1263$. The Sacker-Sell spectrum in this example is $\sigma_{\mathrm{ED}} = [-\sigma_4, \sigma_2] \cup [-\sigma_1, \sigma_3]$.

4.2 Homoclinic orbits

We apply our algorithm to the variational equation along a homoclinic orbit

$$\bar{x}_{n+1} = f(\bar{x}_n),\ n \in \mathbb{Z}, \quad \lim_{n \to \pm\infty} \bar{x}_n = \xi_-.$$

This example only exhibits point spectrum

$$\sigma_{\mathrm{ED}} = \{-\sigma_1, \sigma_2\}.$$

Figures 7, 8 and Table 3 show the resulting output of our algorithms.

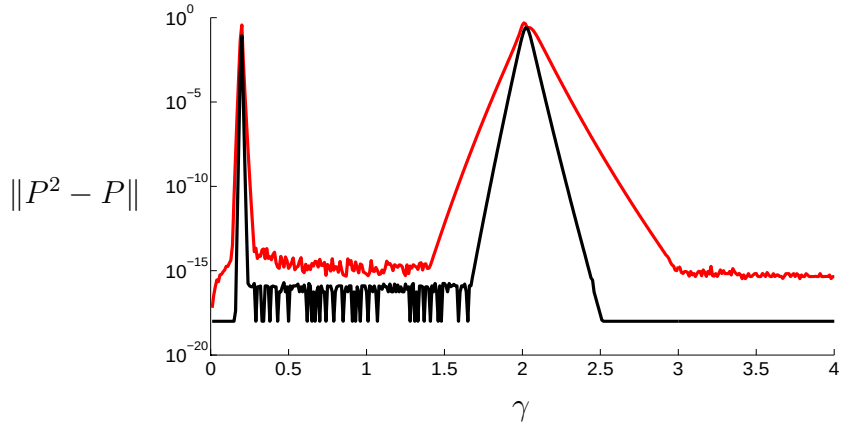

Figure 7: *Detection of Sacker-Sell spectrum for the variational equation along a homoclinic Hénon orbit. Projector residual of the least squares ansatz in red and of the boundary value approach in black.*

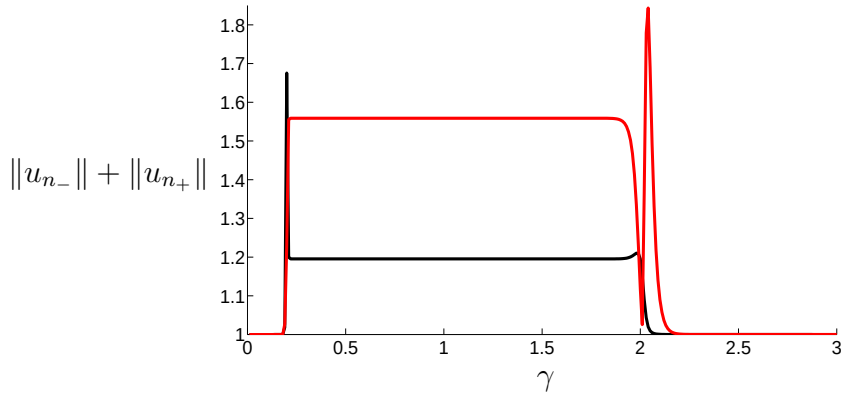

Figure 8: *Detection of Sacker-Sell spectrum for the variational equation along a homoclinic Hénon orbit, via the second approach, applied to the original equation (black) and the adjoint equation (red).*

$\pm n_\pm$		
100	[0.188, 0.206]	[1.994, 2.081]
500	[0.195, 0.198]	[2.029, 2.046]
2000	[0.196, 0.196]	[2.036, 2.039]

Table 3: *Computation of spectral intervals along a homoclinic orbit with a sampling of* γ *in* 0.001 *steps and* $\varepsilon = 0.1$*, using the midpoints* $u_{n_{1,2}}$.

4.3 An orbit on the attractor

We construct a chaotic orbit on the Hénon attractor for the classical parameters $a = 1.4$, $b = 0.3$ by iterating a suitable initial point. Then our algorithms are applied to the corresponding variational equation.

In this example, the linearization is not asymptotically constant. It is not known, whether the assumptions from Section 3.2 are satisfied. Using the projector residual, we cannot decide, whether this equation has continuous or discrete spectrum. The only hint is given by the least squares curve that has no plateaus in Figure 9. The output of the second and third approach in Figure 10 and Table 4 suggest that this difference equation has only point spectrum.

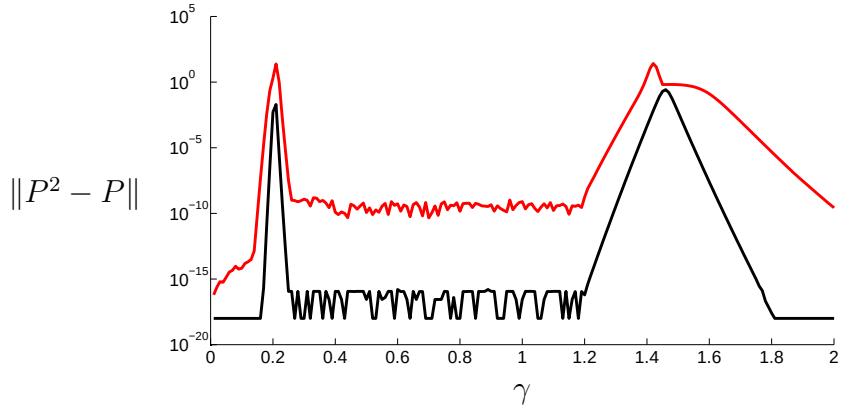

Figure 9: *Detection of Sacker-Sell spectrum for the variational equation along a trajectory on the attractor. Projector residual of the least squares ansatz in red and of the boundary value approach in black.*

$\pm n_\pm$		
100	[0.176, 0.225]	[1.334, 1.650]
500	[0.189, 0.202]	[1.441, 1.529]
2000	[0.199, 0.202]	[1.495, 1.530]

Table 4: *Computation of spectral intervals along a trajectory on the Hénon attractor with a sampling of* γ *in* 0.001 *steps and* $\varepsilon = 0.01$*, using the midpoints* $u_{n_{1,2}}$.

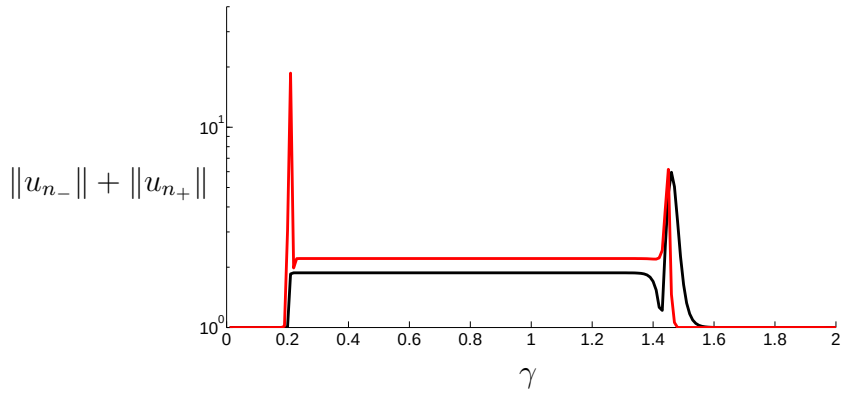

Figure 10: *Detection of Sacker-Sell spectrum for the variational equation along a trajectory on the attractor, via the second approach, applied to the original equation (black) and the adjoint equation (red).*

4.4 Comparison with the QR-approach

We compare our results with the discrete QR-method, combined with Steklov averaging, cf. Dieci & Van Vleck (2002), Dieci & Elia (2008). A rough implementation for computing Sacker-Sell spectra of the difference equation (4) can be written as follows. Choose $Z_{n_-} = I$ and iterate

$$Q_i R_i = Z_i, \quad Z_{i+1} = A_i Q_i, \quad \text{for} \quad i = n_-, \ldots, n_+ - 1,$$

where $Q_i R_i = Z_i$ denotes the unique QR-decomposition of the matrix Z_i, cf. Golub & Van Loan (1996). Let $H > 0$. Compute for $\ell = 1, \ldots, k$ and $m = n_-, \ldots, n_+ - 1 - H$

$$a(\ell, m) = \frac{1}{H} \log \left(\prod_{i=m}^{m+H} R_i(\ell, \ell) \right),$$

define

$$a_-(\ell) = \min_m a(\ell, m), \quad a_+(\ell) = \max_m a(\ell, m),$$

and obtain an approximation of the ℓ-th spectral interval by $\left[\mathrm{e}^{a_-(\ell)}, \ \mathrm{e}^{a_+(\ell)}\right]$.

We repeat the numerical experiments using the QR-method for $\pm n_\pm = 2000$ and $H = 1000$. For Example 6, we obtain in the transversal case the intervals

$$[0.9979, 2.0052], \quad [3.0002, 4.0069], \quad [4.9991, 6.0225],$$

and in the tangential case with $S_2 e_1 = S_1 e_2$ one has

$$[0.9995, 2.0781], \quad [2.8976, 4.0066], \quad [4.9990, 6.0129].$$

One observes that the QR-algorithm, as described above, only detects half-sided dichotomies. In order to detect Sacker-Sell spectrum on the real line, one additionally has to check in case (iii), cf. Section 3.2, whether $\mathcal{R}(P_N^{-u}) \cap \mathcal{R}(P_N^{+s}) \neq \{0\}$. For this task, the authors of Dieci et al. (2010) use an Evans-function approach that is based on computing the determinant of a matrix, consisting of a basis of $\mathcal{R}(P_N^{-u})$ and $\mathcal{R}(P_N^{+s})$. Note that these bases already have been computed in the QR-algorithm.

In the Hénon example, we get the following spectral intervals in case of

- a heteroclinic orbit

$$[0.1260, 0.1963], \quad [2.0372, 3.1721],$$

- a homoclinic orbit

$$[0.1959, 0.1963], \quad [2.0361, 2.0395],$$

- the trajectory on the attractor

$$[0.1934, 0.2036], \quad [1.4718, 1.5494].$$

We do not analyze computing times formally. In our numerical experiments, we observe that the discrete QR-method is relatively cheap, and its numerical effort compares to just a few samples in the boundary value approach.

4.5 Conclusion

We have introduced three approaches for detecting Sacker-Sell spectra that are based on solving linear boundary value problems for γ on a grid. A detailed error analysis is presented. The proposed methods also detect spectral intervals, caused by tangential intersections of the corresponding stable and unstable subspaces of half-sided dichotomies. On the one hand, our methods for detecting the whole Sacker-Sell spectrum are more expensive than QR-techniques, which do not require sampling.

The proposed algorithms are very efficient for scanning small intervals and particularly for analyzing whether a given difference equation has an exponential dichotomy. Using the first algorithm that computes the projector residual, one additionally obtains an accurate approximation of the corresponding stable projector. The second method solves boundary value problems for the original and the adjoint equation, while it suffices to consider the original equation for the third ansatz. In the latter case, Theorem 10 provides precise estimates for the numerically detected Sacker-Sell spectrum with respect to the finite computational interval $[n_-, n_+]$.

Furthermore, the shape of the boundary value solutions (exponential growth towards the end points or the midpoint) provides information on the type of the one-sided dichotomies that lead to spectral intervals.

A Exponential dichotomy

In this appendix, we briefly introduce the notion of an exponential dichotomy, cf. Coppel (1978), Palmer (1988). Consider the linear difference equation

$$u_{n+1} = A_n u_n, \quad n \in \mathbb{Z}, \quad A_n \text{ invertible}, \tag{41}$$

and its solution operator Φ, defined as

$$\Phi(n,m) := \begin{cases} A_{n-1} \dots A_m, & \text{for } n > m, \\ I, & \text{for } n = m, \\ A_n^{-1} \dots A_{m-1}^{-1}, & \text{for } n < m. \end{cases}$$

Definition 11 *The linear difference equation (41) possesses an* ***exponential dichotomy*** *with data $(K, \alpha_s, \alpha_u, P_n^s, P_n^u)$ on $J \subset \mathbb{Z}$, if there exist two families of projectors P_n^s and $P_n^u = I - P_n^s$ and constants $K,\ \alpha_s,\ \alpha_u > 0$, such that the following statements hold:*

$$P_n^s \Phi(n,m) = \Phi(n,m) P_m^s \quad \forall n, m \in J, \tag{42}$$

$$\begin{aligned} \|\Phi(n,m)P_m^s\| &\leq K e^{-\alpha_s (n-m)} \\ \|\Phi(m,n)P_n^u\| &\leq K \mathrm{e}^{-\alpha_u (n-m)} \end{aligned} \quad \forall n \geq m,\ n, m \in J.$$

Exponential dichotomies widely apply in dynamical systems theory. For example when considering connecting orbits of fixed points or homoclinic trajectories, cf. Hüls (2007), of autonomous and non-autonomous difference equations

$$x_{n+1} = f_n(x_n), \quad n \in \mathbb{Z},$$

exponential dichotomies of the variational equation

$$u_{n+1} = Df_n(x_n)u_n, \quad n \in \mathbb{Z}$$

have a geometric interpretation. In the autonomous case stable and unstable manifolds intersect transversally cf. Palmer (1988), while in non-autonomous systems, the same holds true for the corresponding stable and unstable fiber bundles, see Hüls (2006).

Acknowledgement

The author wishes to thank Wolf-Jürgen Beyn for stimulating discussions about this paper. He is grateful to two anonymous referees for several helpful suggestions that improved the first version of this paper.

References

Aulbach, B. & Siegmund, S. (2001), 'The dichotomy spectrum for noninvertible systems of linear difference equations', *J. Differ. Equations Appl.* **7**(6), 895–913. On the occasion of the 60th birthday of Calvin Ahlbrandt.

Beyn, W.-J., Hüls, T., Kleinkauf, J.-M. & Zou, Y. (2004), 'Numerical analysis of degenerate connecting orbits for maps', *Internat. J. Bifur. Chaos Appl. Sci. Engrg.* **14**(10), 3385–3407.

Coppel, W. A. (1978), *Dichotomies in Stability Theory*, Springer-Verlag, Berlin. Lecture Notes in Mathematics, Vol. 629.

Devaney, R. L. (1989), *An Introduction to Chaotic Dynamical Systems*, Addison-Wesley Studies in Nonlinearity, second edn, Addison-Wesley Publishing Company Advanced Book Program, Redwood City, CA.

Dieci, L. & Elia, C. (2008), 'SVD algorithms to approximate spectra of dynamical systems', *Math. Comput. Simulation* **79**(4), 1235–1254.

Dieci, L., Elia, C. & Vleck, E. V. (2010), 'Exponential dichotomy on the real line: SVD and QR methods', *Journal of Differential Equations* **248**(2), 287 – 308.

Dieci, L. & Van Vleck, E. S. (2002), 'Lyapunov spectral intervals: theory and computation', *SIAM J. Numer. Anal.* **40**(2), 516–542 (electronic).

Dieci, L. & Van Vleck, E. S. (2007), 'Lyapunov and Sacker-Sell spectral intervals', *J. Dynam. Differential Equations* **19**(2), 265–293.

Golub, G. H. & Van Loan, C. F. (1996), *Matrix computations*, Johns Hopkins Studies in the Mathematical Sciences, third edn, Johns Hopkins University Press, Baltimore, MD.

Hale, J. K. & Koçak, H. (1991), *Dynamics and Bifurcations*, Vol. 3 of *Texts in Applied Mathematics*, Springer-Verlag, New York.

Hénon, M. (1976), 'A two-dimensional mapping with a strange attractor', *Comm. Math. Phys.* **50**(1), 69–77.

Hüls, T. (2005), 'Bifurcation of connecting orbits with one nonhyperbolic fixed point for maps', *SIAM J. Appl. Dyn. Syst.* **4**(4), 985–1007 (electronic).

Hüls, T. (2006), 'Homoclinic orbits of non-autonomous maps and their approximation', *J. Difference Equ. Appl.* **12**(11), 1103–1126.

Hüls, T. (2007), Homoclinic trajectories of non-autonomous maps, Technical Report 07-011, Bielefeld University, CRC 701. To appear in J. Difference Equ. Appl.

Hüls, T. (2009), 'Numerical computation of dichotomy rates and projectors in discrete time', *Discrete Contin. Dyn. Syst. Ser. B* **12**(1), 109–131.

Mira, C. (1987), *Chaotic dynamics*, World Scientific Publishing Co., Singapore. From the one-dimensional endomorphism to the two-dimensional diffeomorphism.

Palmer, K. J. (1988), Exponential dichotomies, the shadowing lemma and transversal homoclinic points, *in* 'Dynamics reported, Vol. 1', Teubner, Stuttgart, pp. 265–306.

Sacker, R. J. & Sell, G. R. (1978), 'A spectral theory for linear differential systems', *J. Differential Equations* **27**(3), 320–358.

Shinozaki, N., Sibuya, M. & Tanabe, K. (1972), 'Numerical algorithms for the Moore-Penrose inverse of a matrix: direct methods', *Ann. Inst. Statist. Math.* **24**, 193–203.